

# Divalent Ytterbium and Iron Metallocenes of a Dimethyldihydropyrene-Fused Cyclopentadienyl

Wei Fan, David J. Berg,\* Reginald H. Mitchell,\* and Tosha M. Barclay†

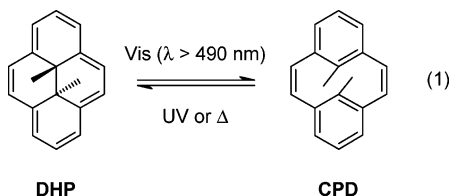
Department of Chemistry, University of Victoria, P.O. Box 3065, Victoria, British Columbia, Canada V8W 3V6

Received March 1, 2007

The photoisomerizable, dimethyldihydropyrene-fused cyclopentadienide salt LiCpDHP reacts with FeCl<sub>2</sub> to form Fe(CpDHP)<sub>2</sub> (**1**). Reaction of the parent cyclopentadiene HCpDHP with Yb[N(SiMe<sub>3</sub>)<sub>2</sub>]<sub>2</sub>[THF]<sub>2</sub> similarly affords the bent ytterbium metallocene Yb(CpDHP)<sub>2</sub>(THF)<sub>2</sub> (**3**). Both metallocenes are formed as a mixture of *rac* and *meso* isomers in 3:2 and 1:1 ratios for Fe and Yb, respectively. NMR data are consistent with η<sup>5</sup>-coordination of the CpDHP ligand in **1**, and this is also confirmed to be the case in **3** by X-ray crystallography. Attempts to oxidize the Yb(II) center in **3** with *p*-tolylidysulfide led to loss of the CpDHP ligand as the dimer (CpDHP)<sub>2</sub>. Photolysis of either **1** or **3** at wavelengths longer than 490 nm did not result in isomerization to the ring-opened cyclophanediene form of the ligand, in contrast to the lithium salt LiCpDHP.

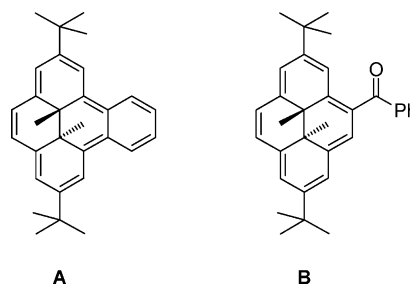
## Introduction

Highly colored dimethyldihydropyrenes (DHP) undergo photoisomerization to colorless, open cyclophanedienes (CPD) on irradiation by visible light (λ > 490 nm), prompting interest in this class of compounds for potential use in optical data storage and photoswitches (eq 1).<sup>1</sup>



However, the thermal or photochemical (UV) reverse reaction often takes place in hours or days, limiting the practical usefulness of the DHP photochrome in real devices. A wide range of organic derivatives of DHP have been prepared,<sup>1b,2</sup> and some of these such as the [*e*]-fused benzo derivative (**A**) and those bearing acyl groups (**B**) show improved photo-opening and slower thermal closing properties.

Metal π-complexes of the DHP system are an interesting alternative to organic functionalization because the bonding mode between the metal and the DHP core is completely different. This may result in enhanced or diminished photochromic properties for the resulting complexes, but the potential range of behavior should be greater than that observed in organic systems alone. Redox-active metals may display electrochromic



behavior as well as DHP-based photochromism, adding another dimension to the switching ability of such complexes; in fact, this dual behavior has already been realized in (BenzoDHP)-Ru(C<sub>5</sub>Me<sub>5</sub>)<sup>+</sup>PF<sub>6</sub><sup>-</sup>.<sup>3</sup> In cases where the metal complex displays improved photochromic properties, variation of the ligands within the metal coordination sphere offers potential for fine-tuning the photochemistry further. Ultimately, polymeric systems where DHP groups bridge between metal centers may offer photoactive polymers where the color is dependent on the metal oxidation state.

The synthesis of metallocenes based on [*e*]-cyclopentadienyl-fused DHP (CpDHP) is reported here. The synthesis of HCpDHP and its lithium salt, LiCpDHP, was reported by us previously.<sup>4</sup> The effect of a fused Cp on the aromaticity of the [14]annulene DHP core was found to be similar to that of benzene in benzoDHP (**A**), and as hoped, LiCpDHP is itself photochromic.<sup>4</sup> The planar and bent metallocenes of Fe(II) and Yb(II), respectively, are discussed in detail here; mono-CpDHP derivatives of other metals will be discussed in a forthcoming publication. The ferrocene derivative of CpDHP is a natural first step into this chemistry given the high thermal and air stability of ferrocene itself. In contrast, the ytterbocene derivative may seem an unusual representative of the bent metallocenes, but the steric bulk of CpDHP is well-suited to the large Yb(II) metal center and attempts to prepare bent metallocenes of the

\* Corresponding authors. E-mail: djberg@uvic.ca; regmitch@uvic.ca.  
† North Harris College, 2700 W.W. Thorne Dr., Houston, TX 77073-3499.

(1) (a) Mitchell, R. H. *Eur. J. Org. Chem.* **1999**, 2695. (b) Mitchell, R. H.; Ward, T. R.; Chen, Y.; Wang, Y.; Weerawarna, S. A.; Dibble, P. W.; Marsella, M. J.; Almutairi, A.; Wang, Z. *J. Am. Chem. Soc.* **2003**, *125*, 2974. (c) Liddell, P. A.; Kodis, G.; Andréasson, J.; de la Garza, L.; Bandyopadhyay, S.; Mitchell, R. H.; Moore, T. A.; Moore, A. L.; Gust, D. *J. Am. Chem. Soc.* **2004**, *126*, 4803.

(2) (a) Sheepwash, M. A. L.; Ward, T. R.; Wang, Y.; Bandyopadhyay, S.; Mitchell, R. H.; Bohne, C. *Photochem. Photobiol. Sci.* **2003**, *2*, 104. (b) Sheepwash, M. A. L.; Mitchell, R. H.; Bohne, C. *J. Am. Chem. Soc.* **2002**, *124*, 4693.

(3) Mitchell, R. H.; Brkic, Z.; Sauro, V. A.; Berg, D. J. *J. Am. Chem. Soc.* **2003**, *125*, 7581.

(4) Mitchell, R. H.; Fan, W.; Lau, D. Y. K.; Berg, D. J. *J. Org. Chem.* **2004**, *69*, 549.

group 4 metals met with failure. The fact that both planar and bent metallocenes are accessible for CpDHP shows the versatility of this ligand and its suitability in forming metal complexes of the DHP system.

## Experimental Section

**General Procedures.** All reactions were carried out under a nitrogen atmosphere, with the exclusion of water and oxygen, using glovebox (Braun MB150-GII) or vacuum line techniques. Tetrahydrofuran (THF), diethyl ether, hexane, and toluene were dried by distillation from sodium benzophenone ketyl under argon immediately prior to use.  $\text{Yb}[\text{N}(\text{SiMe}_3)_2][\text{THF}]_2$ <sup>5</sup> and 2,7-di-*tert*-butyl-*trans*-11c,11d-dimethyl-11c,11d-dihydro-9*H*-cyclopenta[*e*]pyrene (HCpDHP)<sup>4</sup> were prepared as previously reported.

NMR spectra were recorded using a Bruker Avance-500 MHz spectrometer: <sup>1</sup>H (500.13 MHz) and <sup>13</sup>C (125.8 MHz) unless otherwise specified. All deuterated solvents were dried over activated 4 Å molecular sieves except for *d*<sub>8</sub>-tetrahydrofuran (*d*<sub>8</sub>-THF), which was dried by distillation from sodium benzophenone ketyl under argon and stored over activated 4 Å molecular sieves. The spectra were recorded using 5 mm tubes fitted with a Teflon valve (Brunfeldt) at room temperature unless otherwise specified and were referenced to residual solvent resonances. Melting points were recorded using a Büchi melting point apparatus in sealed capillary tubes and are not corrected. Despite the use of co-oxidants such as V<sub>2</sub>O<sub>5</sub> and PbO<sub>2</sub>, the analytical data for most complexes were consistently low in carbon. Mass spectra were recorded on a Kratos Concept H spectrometer using liquid secondary ion ionization (LSIMS).

**(CpDHP)<sub>2</sub>Fe (1). Method A:** A solution of HCpDHP (0.057 g, 0.15 mmol) and LiCH<sub>2</sub>SiMe<sub>3</sub><sup>6</sup> (0.014 g, 0.15 mmol) in 5 mL of toluene was stirred overnight in the glovebox. Solid FeCl<sub>2</sub> (0.009 g, 0.08 mmol) was then added followed immediately by a few drops of THF. The resulting deep green suspension was stirred overnight at room temperature and then taken to dryness under reduced pressure. The residue was extracted into hot hexane, filtered through Celite, and crystallized by slow cooling to room temperature to give **1** as dark brown crystals. Yield: 0.019 g, 29%. Mp: dec (does not melt below 350 °C). NMR<sup>†</sup> (*d*<sub>8</sub>-THF): major isomer <sup>1</sup>H δ 7.31 (d, *J* = 1.4 Hz, 2H, H-8/1), 7.03 (d, *J* = 1.4 Hz, 2H, H-1/8), 6.67 (s, 2H, H-3/6), 6.65 (s, 2H, H-6/3\*), 6.36–6.40 (m, 4H, H-4 and H-5\*), 5.03 (dd, *J* = 2.4, 0.8 Hz, 2H, H-9/11), 4.78 (dd, *J* = 2.4, 0.8 Hz, 2H, H-11/9), 4.02 (t, *J* = 2.4 Hz, 2H, H-10), 1.35 (s, 18H, *t*-Bu-2/7), 1.29 (s, 18H, *t*-Bu-7/2), 0.66 (s, 6H, Me-11c/d), –0.57 (s, 6H, Me-11d/c); <sup>13</sup>C{<sup>1</sup>H} δ 145.50 (C-2 and C-7), 141.79, 140.96, 139.89\*, 138.83 (C-3a, C-5a, C-11b and C-11e), 121.56, 121.52 (C-4 and C-5), 119.22, 119.13 (C3 and C6), 118.72\*, 118.29 (C-1 and C-8), 84.03, 82.81 (C-11a and C-11f), 74.05 (C-10), 67.97, 65.49 (C-9 and C-11), 41.63, 40.20 (C-11c and C-11d), 35.51, 35.41 (CMe<sub>3</sub>), 30.54\*, 30.44 (CMe<sub>3</sub>), 25.86 (*endo*-CH<sub>3</sub>), 20.07 (*exo*-CH<sub>3</sub>); minor isomer <sup>1</sup>H δ 7.28 (d, *J* = 1.4 Hz, 2H, H-8/1), 7.19 (d, *J* = 1.4 Hz, 2H, H-1/8), 6.68 (s, 2H, H-3/6), 6.65 (s, 2H, H-6/3\*), 6.36–6.40 (m, 4H, H-4/5\*), 5.08 (dd, *J* = 2.4, 0.8 Hz, 2H, H-9/11), 4.88 (dd, *J* = 2.4, 0.8 Hz, 2H, H-11/9), 3.78 (t, *J* = 2.4 Hz, 2H, H-10), 1.342 (s, 18H, *t*-Bu-2/7), 1.340 (s, 18H, *t*-Bu-7/2), 0.65 (s, 3H, Me-11c/d), –0.55 (s, 3H, Me-11d/c); <sup>13</sup>C{<sup>1</sup>H} δ 145.63, 145.54 (C-2 and C-7), 141.61, 141.16, 139.89\*, 138.52 (C-3a, C-5a, C-11b and C-11e), 121.65, 121.58 (C-4 and C-5), 119.32, 119.08 (C3 and C6), 118.72\*, 117.98 (C-1 and C-8), 83.32, 83.15 (C-11a and C-11f), 75.10 (C-10), 68.18, 64.64 (C-9 and C-11), 41.70, 40.37 (C-11c and C-11d), 35.48, 35.47 (CMe<sub>3</sub>), 30.54\*, 30.48 (CMe<sub>3</sub>), 25.14 (*endo*-CH<sub>3</sub>), 20.04 (*exo*-CH<sub>3</sub>). †A slash indicates uncertain assignments; for example, H9/11 indicates either H9 or H11. \*An

asterisk indicates overlapping major and minor isomer resonances. IR (KBr disk): ν 3018 (w), 2961 (vs), 2863 (s), 1627 (m), 1458 (br m), 1380 (w), 1360 (s), 1340 (w), 1260 (s), 1225 (m), 1190 (w), 1093 (br s), 1023 (br s), 879 (m), 865 (m), 803 (s), 675 (m) cm<sup>-1</sup>. LRMS (LSIMS): *m/z* 818 (M<sup>+</sup>, 60%), 803 (M<sup>+</sup> – CH<sub>3</sub>, 8%), 788 (M<sup>+</sup> – 2CH<sub>3</sub>, 30%), 773 (M<sup>+</sup> – 3CH<sub>3</sub>, 20%), 758 (M<sup>+</sup> – 4CH<sub>3</sub>, 100%), 381 (CpDHP<sup>+</sup>, 73%). HRMS: *m/z* calcd (found) for C<sub>58</sub>H<sub>66</sub>Fe 818.4513 (818.4509). UV–vis (cyclohexane): λ<sub>max</sub> (ε<sub>max</sub>) 289 (3.8 × 10<sup>5</sup>), 410 (2.6 × 10<sup>5</sup>) nm with an extended tail to 800 nm. Anal. Calcd for C<sub>58</sub>H<sub>66</sub>Fe: C, 85.06; H, 8.12. Found: C, 83.42; H, 7.53.

**Method B:** In this variation, FeCl<sub>2</sub> (0.038 g, 0.30 mmol), LiCH<sub>2</sub>SiMe<sub>3</sub> (0.038 g, 0.40 mmol) and HCpDHP (0.152 g, 0.40 mmol) were placed together in a Kontes flask under argon on a vacuum line and dissolved in a mixture of THF and toluene (10 mL and 2 mL). The deep green solution was stirred rapidly overnight and the solvent was then removed under vacuum. The flask was transferred to the glovebox and the residue was extracted with hot hexane, filtered and the filtrate cooled to room temperature to afford **1** as dark brown crystals. Yield: 0.016 g, 10%.

**(CpDHP)Fe(Cp) (2).** Reaction of an equimolar mixture of LiCp and LiCpDHP with FeCl<sub>2</sub> following a similar procedure to method A above yielded a small amount of brown solid. <sup>1</sup>H NMR analysis of this material revealed that it was a mixture of ferrocene **1** and the mixed ligand species **2**. Separation of this mixture was not successful, and attempts to prepare **2** from a Cp-containing precursor such as CpFe(CO)<sub>2</sub>I failed. Partial characterization of this compound by <sup>1</sup>H NMR spectroscopy is given below. NMR (*d*<sub>6</sub>-benzene): <sup>1</sup>H δ 7.28 (br s, 1H, H-8/1), 7.20 (br s, 1H, H-1/8), 6.79 (br s, 1H, H-6/3), 6.72 (br s, 1H, H-3/6), 6.42 (s, 1H, H-5/4), 6.15 (m, 1H, H-4/5), 4.98 (br s, 1H, H-11/9), 4.93 (br s, 1H, H-9/11), 4.10 (m, 1H, H-10), 3.93 (s, 5H, Cp-H), 1.32 (s, 18H, *t*-Bu-2 and *t*-Bu-7), 0.81 (s, 3H, Me-11c/d), 0.01 (s, 3H, Me-11d/c).

**(CpDHP)<sub>2</sub>Yb(THF)<sub>2</sub> (3).** A solution of HCpDHP (0.078 g, 0.20 mmol) in 5 mL of toluene was prepared in a nitrogen-filled glovebox and added to a solution of Yb[N(SiMe<sub>3</sub>)<sub>2</sub>][THF]<sub>2</sub> (0.064 g, 0.10 mmol) by Pasteur pipet. The resulting dark green solution was stirred at room temperature for 2 days and filtered through Celite on a glass frit, and the filtrate was taken to dryness under reduced pressure. The residue was recrystallized from hot hexane to afford **3** as dark red crystals. Yield: 0.032 g, 30%. Mp: 210 °C (dec). NMR (*d*<sub>8</sub>-THF): isomer A <sup>1</sup>H δ 7.93 (s, 2H, H-8/1), 7.46 (s, 2H, H-6/3), 7.15 (s, 2H, H-1/8), 6.98 (s, 2H, H-3/6), 6.94 (br s, 2H, H-9/11), 6.83–6.89 (m, 4H, H-4 and H-5\*), 6.61 (d, *J* = 1.9 Hz, 2H, H-9/11), 5.71–5.73 (m, 2H, H-10\*), 1.61 (s, 18H, *t*-Bu-2/7), 1.38 (s, 18H, *t*-Bu-7/2), –1.07 (br s, 6H, Me-11c/d\*), –1.56 (s, 6H, Me-11d/c); <sup>13</sup>C{<sup>1</sup>H} δ 145.35, 144.72 (C-2 and C-7), 139.94, 138.61 (C-3a and C-5a), 137.15 (C-11b and C-11e, overlapping), 122.23, 121.94 (C-11a and C-11f), 120.02, 119.98 (C4 and C5), 116.78, 116.34\* (C-3 and C-6), 114.00 (C-10), 112.76, 112.37 (C-1 and C-8), 102.85, 101.45\* (C-9 and C-11), 39.40, 37.33 (C-11c and C-11d), 36.11, 35.97 (CMe<sub>3</sub>), 31.67, 31.30 (CMe<sub>3</sub>), 19.97 (*endo*-CH<sub>3</sub>), 18.86 (*exo*-CH<sub>3</sub>); isomer B <sup>1</sup>H δ 7.72 (s, 2H, H-8/1), 7.69 (s, 2H, H-1/8), 7.08 (s, 2H, H-6/3), 7.02 (s, 2H, H-3/6), 6.83–6.89 (m, 4H, H-4/5\*), 6.81 (br s, 2H, H-9/11), 6.72 (br s, 2H, H-11/9), 5.71–5.73 (m, 2H, H-10), 1.50 (s, 18H, *t*-Bu-2/7), 1.49 (s, 18H, *t*-Bu-7/2), –1.07 (s, 6H, Me-11c/d\*), –1.52 (s, 6H, Me-11d/c); <sup>13</sup>C{<sup>1</sup>H} δ 145.11, 144.86 (C-2 and C-7), 139.78, 138.88 (C-3a and C-5a), 137.43, 136.92 (C-11b and C-11e), 122.15, 121.87 (C-11a and C-11f), 120.13, 119.90 (C4 and C5), 116.98, 116.34\* (C-3 and C-6), 113.65 (C-10), 112.79, 112.54 (C-1 and C-8), 103.04, 101.45\* (C-9 and C-11), 39.56, 37.36 (C-11c and C-11d), 35.81 (CMe<sub>3</sub>, overlapping), 31.52, 31.42 (CMe<sub>3</sub>), 20.06 (*endo*-CH<sub>3</sub>), 18.97 (*exo*-CH<sub>3</sub>). Anal. Calcd for C<sub>66</sub>H<sub>82</sub>O<sub>2</sub>Yb (bis-THF solvate): C, 73.37; H, 7.65. Anal. Calcd for C<sub>62</sub>H<sub>74</sub>OYb (mono-THF solvate): C, 73.85; H, 7.40. Anal. Calcd for C<sub>58</sub>H<sub>66</sub>Yb (THF-free complex): C, 74.41; H, 7.11. Found: C, 72.92; H, 7.21.

(5) Tilley, T. D.; Zalkin, A.; Andersen, R. A.; Templeton, D. H. *Inorg. Chem.* **1981**, *20*, 551.

(6) Tessier-Youngs, C.; Beachley, O. T., Jr. *Inorg. Synth.* **1986**, *24*, 95.

**Table 1.** Summary of Crystallographic Data for 3·Hexane<sup>a</sup>

formula	YbO <sub>2</sub> C <sub>72</sub> H <sub>96</sub>	2θ range (deg)	4–50
fw (g mol <sup>-1</sup> )	1165.3	F000	2456
cryst size (mm)	0.23 × 0.33 × 0.36	linear abs coeff (mm <sup>-1</sup> )	1.56
a (Å)	19.010(3)	no. of reflns measd	25 292
b (Å)	15.518(2)	no. of unique reflns	10 605
c (Å)	22.079(3)	no. of reflns > 2σ(I)	7101
β (deg)	109.142(3)	no. of params refined	745
V (Å <sup>3</sup> )	6153(2)	no. of params restrained	18
calc density (g cm <sup>-3</sup> )	1.26	R1 <sup>b</sup> , wR2 <sup>c</sup>	0.035, 0.071
space group	P2 <sub>1</sub> /n	R1 <sup>b</sup> all data	0.064
Z	4	GOF	0.92

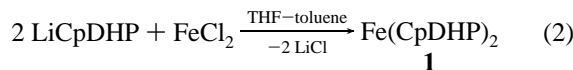
<sup>a</sup> Collected at 223 K using Mo Kα radiation (λ = 0.71073 Å). <sup>b</sup> R = Σ(|F<sub>o</sub>| - |F<sub>c</sub>|)/Σ|F<sub>o</sub>|. <sup>c</sup> R<sub>w</sub> = [Σw(|F<sub>o</sub>| - |F<sub>c</sub>|)<sup>2</sup>/Σw(|F<sub>o</sub>|)<sup>2</sup>]<sup>1/2</sup>.

(CpDHP)<sub>2</sub> (**4**). Attempts to oxidize **3** with one-half of an equivalent of *p*-tolyl disulfide in toluene initially produced a deep purple solution, but this color rapidly faded to greenish-brown within minutes. Removal of solvent and recrystallization yielded a deep green hydrocarbon product believed to be the dimer on the basis of mass spectroscopic evidence. LRMS (LSIMS): *m/z* 762 (M<sup>+</sup>, 4%), 747 (M<sup>+</sup> - CH<sub>3</sub>, 2%), 732 (M<sup>+</sup> - 2CH<sub>3</sub>, 4%), 717 (M<sup>+</sup> - 3CH<sub>3</sub>, 3%), 702 (M<sup>+</sup> - 4CH<sub>3</sub>, 6%), 381 (CpDHP<sup>+</sup>, 100%), 366 (CpDHP<sup>+</sup> - CH<sub>3</sub>, 12%), 351 (CpDHP<sup>+</sup> - 2CH<sub>3</sub>, 43%).

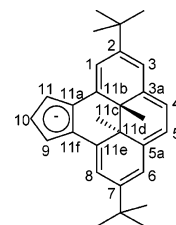
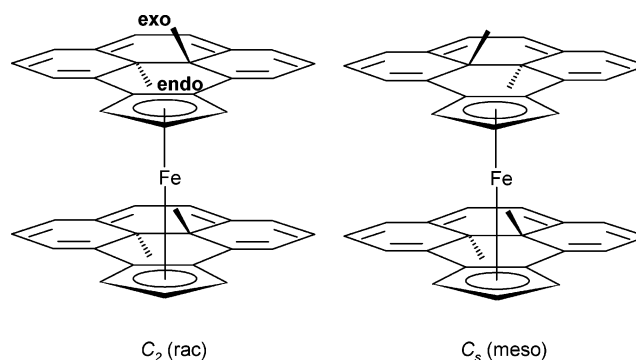
**X-ray Crystallographic Studies.** Crystallographic data for **3** are given in Table 1. A suitable crystal was grown from hot *n*-hexane by slow cooling to room temperature, mounted on a glass fiber under argon, and coated with epoxy to prevent reaction with the atmosphere. The overall decay during data collection was 0.02%. Data were collected on a Siemens Smart 1000 CCD diffractometer equipped with graphite-monochromated Mo Kα radiation (λ = 0.71073 Å) at 223 K. Structure solution was carried out using SHELXS-97,<sup>7</sup> and refinement was done on F<sup>2</sup>. An absorption correction using SADABS was applied (abs range: 0.90–1.00). The final Fourier difference maps showed maximum and minimum peaks of -0.40/+0.82 e Å<sup>-3</sup>. Thermal ellipsoid plots were drawn with ORTEP3.<sup>8</sup> Further details are provided in the Supporting Information.

## Results and Discussion

**Synthesis.** The iron metallocene complex of CpDHP was prepared in low yield by the salt metathesis reaction between preformed LiCpDHP and FeCl<sub>2</sub> (eq 2). The low yield obtained in this reaction may be attributable to the increased steric bulk of CpDHP compared with simple cyclopentadienyl ligands. A one-pot reaction in which 4 equiv of HCpDHP and LiCH<sub>2</sub>SiMe<sub>3</sub> were combined with 3 equiv of FeCl<sub>2</sub> in a THF-toluene mixture and stirred at room temperature overnight afforded ferrocene **1**, albeit in an even poorer yield than the stepwise reaction shown in eq 2 (this stoichiometry gave the best yield). The metallocene structure for **1** was established by HRMS (calcd 818.4513; found 818.4509 amu) and NMR spectroscopy. The brown complex is thermally stable and does not melt below 350 °C, but it decomposes within a few days on exposure to air.



The <sup>1</sup>H and <sup>13</sup>C NMR spectra of **1** clearly show the presence of two isomers in ca. 3:2 ratio. This can be explained by the formation of *meso* and *rac* isomers of C<sub>s</sub> and C<sub>2</sub> symmetry, respectively (Figure 2). The internal methyl resonances on the CpDHP framework of each isomer occur as two well-separated

**Figure 1.** Numbering scheme in CpDHP.**Figure 2.** Isomers of Fe(CpDHP)<sub>2</sub> (**1**).

resonances: one downfield (major isomer, 0.66; minor isomer, 0.67 ppm) and one upfield (-0.57; -0.55 ppm). The upfield resonances are more similar to that observed in the Li<sup>+</sup> salt of the CpDHP<sup>-</sup> anion (-1.82 ppm), suggesting that the downfield resonance corresponds to the *endo* methyl group, which experiences a deshielding effect from the nearby Fe center. The resonance due to H-10 on the Cp ring differs substantially in chemical shift for the two isomers (major, 4.02; minor, 3.78 ppm) but appears as a triplet (<sup>3</sup>J<sub>HH</sub> = 2.4 Hz) in both cases due to equivalent coupling to H-9 and H-11. H-9 and H-11 appear as distinct doublets of doublets in both isomers (<sup>3</sup>J<sub>HH</sub> = 2.4 Hz, <sup>4</sup>J<sub>HH</sub> = 0.8 Hz). It is notable that the chemical shift differences between related, but inequivalent, resonances such as H-9/H-11 and H-1/H-8 and the *t*-Bu resonances at positions 2 and 7 are all greater for the major isomer than for the minor isomer.

The <sup>13</sup>C NMR chemical shifts of the ring junction carbons have been shown to be a sensitive probe of cyclopentadienyl hapticity in indenyl metal complexes.<sup>9</sup> By comparing the difference in ring junction <sup>13</sup>C shifts in transition metal complexes versus the corresponding Na<sup>+</sup> indenide salts (Δδ<sup>13</sup>C), Marder<sup>9a</sup> and Baker<sup>9b</sup> have shown that complexes with crystallographically verified η<sup>5</sup>-Cp ligands show Δδ<sup>13</sup>C between -20 and -40 ppm, while authentic η<sup>3</sup>-Cp ligands show Δδ<sup>13</sup>C values between +5 and +30 ppm. "Slipped" η<sup>5</sup>-Cp complexes

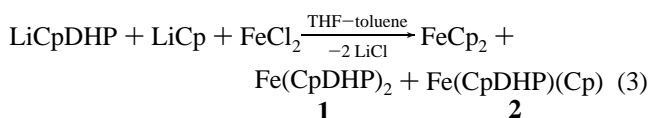
(7) Sheldrick, G. SHELXS-97: Programs for Crystal Structure Determination; University of Göttingen: Germany, 1997.

(8) Farrugia, L. J. ORTEP3 for Windows. *J. Appl. Crystallogr.* **1997**, *30*, 565.

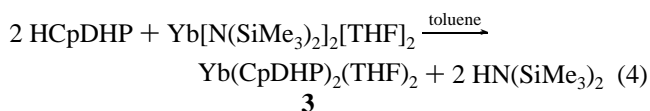
(9) (a) Baker, R. T.; Tulip, T. H. *Organometallics* **1986**, *5*, 839. (b) Westcott, S. A.; Kakkar, A. K.; Stringer, G.; Taylor, N. J.; Marder, T. B. *J. Organomet. Chem.* **1990**, *394*, 777.

showing some distortion toward  $\eta^3$  typically display intermediate  $\Delta\delta^{13}\text{C}$  values of +5 to -20 ppm. In order to make a meaningful comparison in this work, we compared the equivalent ring junction  $^{13}\text{C}$  shifts for C-11a and C-11f with that in LiCpDHP.<sup>4</sup> The average C-11a/C-11f  $\Delta\delta^{13}\text{C}$  values are -39.1 and -39.3 ppm for the major and minor isomers of **1**, respectively. This suggests that the CpDHP ligand is  $\eta^5$ -bonded in **1**, as expected for an  $18\text{e}^-$  metallocene structure.

The mixed cyclopentadienyl metallocene (CpDHP)FeCp (**2**) was prepared by reaction of 1 equiv of LiCpDHP, LiCp, and FeCl<sub>2</sub> in a THF-toluene mixture (eq 3). Not surprisingly, this reaction produced a mixture of ferrocene, **1** and **2**. Attempts to separate **2** from the other products were not entirely successful, but the product was characterized by <sup>1</sup>H NMR. The internal methyl resonances are considerably downfield for both the *endo* (0.81 ppm) and *exo* (0.01 ppm) methyls. This indicates a greatly reduced shielding effect for the Cp ligand relative to another CpDHP. Attempts to prepare **2** more cleanly starting from CpFe(CO)<sub>2</sub>I or to prepare a Cp\* analogue using Cp\*Fe(acac) failed.



A direct acid-base reaction between 2 equiv of HCpDHP and Yb[N(SiMe<sub>3</sub>)<sub>2</sub>]<sub>2</sub>[THF]<sub>2</sub> was used to prepare dark red Yb(CpDHP)<sub>2</sub>(THF)<sub>2</sub> (**3**), eq 4. A salt metathesis reaction between 2 equiv of LiCpDHP and YbI<sub>2</sub> is also possible, but as is often the case in lanthanide chemistry, this reaction produces lower yields and less pure product than the acid-base reaction. In this case, the low yield (30%) was mainly due to the extremely high solubility of **3** in hexane. The identity of **3** was established by NMR and X-ray crystallography (discussed below); mass spectroscopy failed to show a molecular ion, but this may be due to difficulties in introducing the extremely air and moisture sensitive compound into the mass spectrometer.



The <sup>1</sup>H NMR of diamagnetic **3**, like that of **1**, shows evidence for two isomers (Figure 2), although in this case they are in approximately equal ratio. The internal methyls appear as three resonances of 6:3:3 relative integration at -1.07, -1.52, and -1.56 ppm. This pattern is similar to that observed for **1** except that the downfield resonance for the two isomers is overlapping in this case. Therefore, following the assignments for **1**, we assign the overlapping resonance at -1.07 ppm to the *endo* methyls and the separate resonances at -1.52 and -1.56 ppm to the *exo* methyls of the two isomers of **3**. Most notably, *all* internal methyl resonances are further upfield than those in **1**. This is not unexpected because the much larger size of Yb(II) relative to Fe(II) (ionic radii: 1.02 vs 0.61 Å in six-coordination)<sup>10</sup> places the internal methyls much farther away from the metal center and the adjacent CpDHP ring in **3** than in **1**. It is also worth noting that the relative magnitude of the *endo* methyl shielding is greater than the *exo* methyl shielding when comparing **3** to **1** ( $\Delta\delta_{\text{endo}} = -1.73$  ppm vs  $\Delta\delta_{\text{exo}} = -0.98$  ppm). This observation is consistent with the assignments because the *endo* methyls should indeed be more sensitive to changes in metal-ligand and interligand distances.

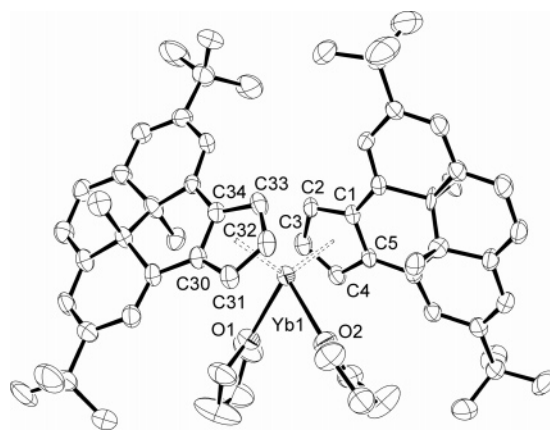


Figure 3. ORTEP38 plot (30% probability ellipsoids) of **3**.

Table 2. Selected Bond Distances (Å) and Angles (deg) for **3**<sup>a</sup>

Bond Distances			
Yb(1)–O(1)	2.432(3)	Yb(1)–O(2)	2.441(3)
Yb(1)–C(1)	2.825(4)	Yb(1)–C(2)	2.701(4)
Yb(1)–C(3)	2.700(4)	Yb(1)–C(4)	2.789(4)
Yb(1)–C(5)	2.872(4)	Yb(1)–Cp <sup>1</sup>	2.505
Yb(1)–C(30)	2.862(4)	Yb(1)–C(31)	2.776(4)
Yb(1)–C(32)	2.691(4)	Yb(1)–C(33)	2.692(4)
Yb(1)–C(34)	2.811(4)	Yb(1)–Cp <sup>2</sup>	2.494
Bond Angles			
O(1)–Yb(1)–O(2)	79.47(10)	O(1)–Yb(1)–Cp <sup>1</sup>	105.8
O(1)–Yb(1)–Cp <sup>2</sup>	111.6	O(2)–Yb(1)–Cp <sup>1</sup>	112.5
O(2)–Yb(1)–Cp <sup>2</sup>	105.4	Cp <sup>1</sup> –Yb(1)–Cp <sup>2</sup>	130.6

<sup>a</sup> Estimated standard deviations in parentheses; Cp<sup>1</sup> and Cp<sup>2</sup> are the centroids of C(1)–C(5) and C(30)–C(34), respectively.

The <sup>13</sup>C NMR spectrum of **3** shows significant differences in chemical shift from **1**, especially for the carbons of the Cp ring. This is not unexpected because the bonding in the Yb(II)–Cp bond is essentially ionic, while the Fe(II)–Cp bond is largely covalent. The resonances for C-9/11 and C-10 are observed at 102.9/101.5 and 114.0 ppm, respectively, in **3** and at 99.1 and 112.6 in LiCpDHP.<sup>4</sup> On the other hand, these same resonances in **1** are found far upfield at 66.6 and 74.6 ppm (average values). The standard explanation for this is that there is considerable  $\pi$ -donation from the Cp to Fe in **1**, which reduces the Cp ring current and results in an upfield shift. In this sense, the CpDHP in **3** behaves much more as a true CpDHP<sup>-</sup> anion with little charge transfer to Yb. The <sup>13</sup>C ring junction shifts used earlier to assess the bonding mode of the Cp ligand are dependent on changes in electron density within the Cp ring caused by changes in hapticity. Inasmuch as the Cp ring in **3** behaves like an anion, these criteria would not be expected to hold and there should be little difference in  $\Delta\delta^{13}\text{C}$  for **3** compared with LiCpDHP itself. In fact, this is the case, as  $\Delta\delta^{13}\text{C}$  for **3** is just -0.5 ppm. Using the criteria established by Baker and Marder, this would indicate a “slipped”  $\eta^5$ -bonding mode, but a close examination of structural parameters for **3** in the next section shows that this description is not warranted.

**Structural Studies of 3.** The X-ray structure of **3** is shown in Figure 3, and crystal data and important bond lengths and angles are given in Tables 1 and 2, respectively. The complex adopts a highly distorted pseudotetrahedral bent metallocene structure. Although C<sub>s</sub> (*meso*) and C<sub>2</sub> (*rac*) isomers of **3** are observed in solution, the solid-state structure possesses no symmetry and the internal methyl positions are disordered; only one contributor to the disorder model is shown in Figure 3.

The Yb(II) center in **3** is formally eight-coordinate and both CpDHP rings are  $\eta^5$ -bonded to the metal. The average  $\eta^5 \rightarrow \eta^3$

(10) Shannon, R. D. *Acta Crystallogr. A* **1976**, *32A*, 751.

“slip” parameter  $\Delta$ , defined as the difference in M–C bond distance for the ring junction and adjacent allylic carbons, is 0.104 Å for **3**. By comparison, complexes containing true  $\eta^3$ -indenyls such as those of the  $[\text{Fe}(\eta^3\text{-Ind})(\text{CO})_3]^-$  anion<sup>11</sup> possess  $\Delta$  values of 0.75 Å or larger. The only other structurally characterized CpDHP complexes,  $(\eta^5\text{-CpDHP})\text{Re}(\text{CO})_3$  and  $(\eta^5\text{-CpDHP})\text{Ru}(\text{C}_5\text{Me}_5)$ ,<sup>12</sup> show similar slip parameters of 0.080 and 0.058 Å, respectively, as do all other Yb(II) indenyl complexes (range: 0.019–0.140 Å).<sup>13</sup>

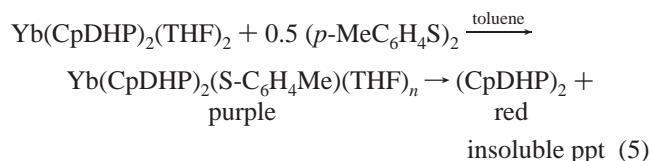
Other measures of indenyl hapticity include the “fold” or “hinge” angles between the allylic or five-membered ring planes and the adjacent benzene ring, respectively. Typically,  $\eta^3$ -indenyls feature fold and hinge angles of more than 20°, while  $\eta^5$ -indenyls have corresponding angles of less than 10° and usually less than 5°.<sup>14</sup> The average fold and hinge angles in **3** are 7.0° and 5.7°, respectively, and well within the range expected for true  $\eta^5$ -coordination. These angles are both slightly greater than those found in other Yb(II) indenyl complexes (fold angle range: 1.4–6.1°; hinge angle range: 0.6–3.7°),<sup>13</sup> but this is probably attributable to greater steric crowding in **3**. In this context, it is noteworthy that  $(\eta^5\text{-CpDHP})\text{Re}(\text{CO})_3$  and  $(\eta^5\text{-CpDHP})\text{Ru}(\text{C}_5\text{Me}_5)$ , possessing smaller metal centers, show even larger hinge and fold angles (fold: 9.0° (Re), 14.7° (Ru); hinge: 7.0° (Re), 13.2° (Ru)).<sup>12</sup>

The torsion angle defined by C3–Cp1<sub>centroid</sub>–Cp2<sub>centroid</sub>–C32, where Cp1<sub>centroid</sub> and Cp2<sub>centroid</sub> refer to the centroid of atoms C1–C5 and C30–C34, respectively, provides one measure of the relative orientation of the CpDHP rings. This angle is 167.8° in **3**, indicating that the rings are staggered relative to one another. This angle varies widely between Yb(II) indenyls (range: 39.9–177.8°), indicating that it is not that sensitive to crowding within the complexes.<sup>13</sup> The wedge angle (Cp1<sub>centroid</sub>–Yb–Cp2<sub>centroid</sub>) and average Yb–C distance are a better guide to crowding in **3** and Yb(II) indenyls generally. By both measures, **3** is slightly more crowded than Yb(Ind)<sub>2</sub>(THF)<sub>2</sub>: the average wedge angle in **3** is 130.6° and the average Yb–C distance is 2.77 Å compared with 128.7° and 2.729 Å for Yb(Ind)<sub>2</sub>(THF)<sub>2</sub>.<sup>13a</sup>

Bond localization within the [14]-annulene ring of DHP by a fused aromatic group has been observed before in benzoDHP<sup>2a</sup> and in  $(\eta^5\text{-CpDHP})\text{Re}(\text{CO})_3$  and  $(\eta^5\text{-CpDHP})\text{Ru}(\text{C}_5\text{Me}_5)$ .<sup>12</sup> Bond alternation around the DHP core can be assessed as  $\Delta\Sigma$  = average “long” – average “short” bond. By this measure the bond length alternation in **3** is slightly lower ( $\Delta\Sigma$  = 0.065 Å) than in either  $(\eta^5\text{-CpDHP})\text{Re}(\text{CO})_3$  or  $(\eta^5\text{-CpDHP})\text{Ru}(\text{C}_5\text{Me}_5)$  ( $\Delta\Sigma$  = 0.077 and 0.070 Å, respectively). By comparison the bond length alternation in [e]-fused benzoDHP is 0.071 Å.<sup>2a</sup>

**Oxidation of (CpDHP)<sub>2</sub>Yb(THF)<sub>2</sub>.** Organometallic compounds of Yb(II) such as Yb(C<sub>5</sub>Me<sub>5</sub>)<sub>2</sub>(Et<sub>2</sub>O) are relatively good reducing agents ( $\epsilon^\circ_{1/2}$  vs SCE = +1.35 V in THF)<sup>15</sup> capable of

reducing organic substrates such as dichalcogenides (RE–ER, E = O, S, Se, Te) and some nitrogen heterocycles (e.g., 2,2′-bipyrimidine).<sup>16,17</sup> With this in mind, we attempted to reduce *p*-tolylsulfide with **3** to form the Yb(III) thiolate complexes shown in eq 5. The reaction mixture immediately turned an intense purple color on combination of the reactants, very similar to the deep blue-purple of Yb(C<sub>5</sub>Me<sub>5</sub>)<sub>2</sub>(S-*p*-tol)(Et<sub>2</sub>O) formed when Yb(C<sub>5</sub>Me<sub>5</sub>)<sub>2</sub>(Et<sub>2</sub>O) reacts with *p*-tolylsulfide.<sup>16</sup> However, in this case the purple color fades within minutes to a greenish-brown, and the only soluble product isolated from the reaction mixture was hydrocarbon. The mass spectrum of this product showed peaks at 762 and 381 amu corresponding to the dimer and monomer of CpDHP, respectively. In addition, the <sup>1</sup>H NMR showed a broad envelope of resonances between –3.0 and –3.6 ppm, consistent with the formation of several isomers of free (CpDHP)<sub>2</sub>. It should be noted that the mass of hydrocarbon obtained from the soluble fraction accounts for about 90% of the mass of the ligand used, clearly ruling out simple precipitation of an insoluble Yb(III) product. Interestingly, attempts to prepare Yb(III) complexes by direct salt metathesis of LiCpDHP with YbCl<sub>3</sub> also produced the same product, perhaps suggesting that Yb(III) CpDHP complexes are inherently unstable.



**Photochemical Reactivity.** LiCpDHP, like most organic DHP derivatives, undergoes photochemical ring opening with visible light ( $\lambda > 490$  nm) to produce the cyclophanediene isomer LiCpCPD (eq 6). One of the goals of this research program is to determine the effect of metal complexation on the opening (forward) and UV or thermal closing (reverse) reaction. Irradiation of **1** or **3** was carried out on a sealed sample in a NMR tube in the absence of air using a 500 W tungsten lamp fitted with a 490 nm (orange) filter. The samples were placed within a cold water jacket in order to minimize the thermal return reaction. Prolonged irradiation of **1** or **3** failed to produce any change in the <sup>1</sup>H NMR (the internal methyls of CPD complexes shift dramatically downfield by 2–4 ppm) or UV/vis spectra, clearly indicating that these complexes do not photoisomerize. In comparison, both  $(\eta^5\text{-CpDHP})\text{Re}(\text{CO})_3$  and  $(\eta^5\text{-CpDHP})\text{Ru}(\text{C}_5\text{Me}_5)$  do undergo ring opening under these conditions.<sup>12</sup> Other iron complexes with one or two Fe(CO)<sub>3</sub> groups bonded directly to the DHP core<sup>18</sup> or with ferrocenyl substituents  $\sigma$ -bonded to the DHP framework<sup>19</sup> are also photochemically inert under these conditions.

The reasons for these differences are not entirely clear, although the fact that **1** possesses a UV/vis peak at 410 nm with a substantial tail out to 800 nm suggests that energy may be lost to ligand field absorptions of the ferrocene unit. In the case of **3**, intense MLCT absorptions, commonly observed in the visible spectra of Yb(II) complexes,<sup>20</sup> are probably responsible for the lack of photoisomerization. This is indirectly

(11) Forschner, T. C.; Cutler, A. R.; Kullnig, R. K. *Organometallics* **1987**, 6, 889.

(12) Fan, W. Ph.D. Thesis; University of Victoria: Victoria, B.C. Canada, 2005.

(13) (a) Yb(Ind)<sub>2</sub>(THF)<sub>2</sub>: Marsh, R. E. *Acta Crystallogr. B* **1997**, 53B, 317. (b) Yb(1-cyclopentylind)<sub>2</sub>(THF)<sub>2</sub>: Qi, M.; Shen, Q.; Gong, X.; Shen, Z.; Weng, L. *Chin. J. Chem.* **2002**, 20, 564. (c) Yb[1-*t*-BuNSiMe<sub>2</sub>Ind]<sub>2</sub>(bipy): Trifonov, A. A.; Spaniol, T. P.; Okuda, J. *Eur. J. Inorg. Chem.* **2003**, 926. (d) Yb(Ind)<sub>2</sub>(2,6-*i*-Pr<sub>2</sub>-Ph-NACNAC)(THF): Yao, Y.; Zhang, Y.; Zhang, Z.; Shen, Q.; Yu, K. *Organometallics* **2003**, 22, 2876. (e) Yb(Ind)(DME)<sub>2</sub>: Trifonov, A. A.; Kirillov, E. N.; Dechert, S.; Schumann, H.; Bochkarev, M. N. *Eur. J. Inorg. Chem.* **2001**, 3055.

(14) (a) Faller, J. W.; Crabtree, R. H.; Habib, A. *Organometallics* **1985**, 4, 929. (b) Trnka, T. N.; Bonanno, J. B.; Bridgewater, B. M.; Parkin, G. *Organometallics* **2001**, 20, 3255.

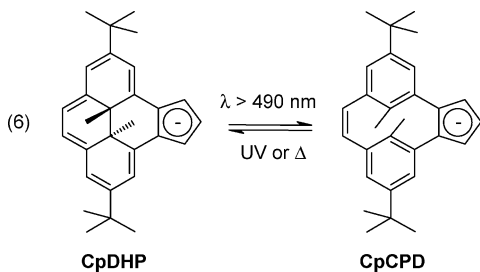
(15) Finke, R. G.; Keenan, S. R.; Schiraldi, D. A.; Watson, P. L. *Organometallics* **1986**, 5, 598.

(16) Berg, D. J.; Andersen, R. A.; Zalkin, A. *Organometallics* **1988**, 7, 1858.

(17) (a) Schultz, M.; Boncella, J. M.; Berg, D. J.; Tilley, T. D.; Andersen, R. A. *Organometallics* **2002**, 21, 460. (b) Walter, M. D.; Schultz, M.; Andersen, R. A. *New J. Chem.* **2006**, 30, 238. (c) Walter, M. D.; Berg, D. J.; Andersen, R. A. *Organometallics* **2006**, 25, 3228.

(18) Zhang, R.; Fan, W.; Twamley, B.; Berg, D. J.; Mitchell, R. H. *Organometallics* **2007**, 26, 1888.

(19) Bandyopadhyay, S. Ph.D. Thesis, University of Victoria: Victoria, B. C. Canada, 2004.



supported by the observation that a very impure sample of  $\text{Y}(\text{CpDHP})_2\text{Cl}$  formed by salt metathesis between  $\text{LiCpDHP}$  and  $\text{YCl}_3$  did undergo photoisomerization.<sup>12</sup> The similarity in bonding between yttrium and ytterbium with Cp-type anions

(20) Brewer, M.; Khasnis, D.; Buretea, M.; Berardini, M.; Emge, T. J.; Brennan, J. G. *Inorg. Chem.* **1994**, *33*, 2743.

but the lack of MLCT transitions for Y(III) supports that these charge-transfer transitions may block Yb(II) photoisomerization. Clearly further study of other lanthanide and transition metal complexes are required before any definitive explanation for the photochemical behavior of DHP-containing metal complexes can be put forward.

**Acknowledgment.** D.J.B. (Discovery Grant) and R.H.M. (Discovery Grant) gratefully acknowledge the support of the Natural Sciences and Engineering Research Council of Canada.

**Supporting Information Available:** Tables of atomic coordinates, bond distances and angles, and anisotropic thermal parameters for **3**;  $^1\text{H}$  NMR spectra of **1** and **3**; and a table summarizing X-ray data for Yb indenides are available free of charge via the Internet at <http://pubs.acs.org>.

OM070194S